Electronic Research Archive

http://www.aimspress.com/journal/era

ERA, 30(12): 4436–4446.
DOI: 10.3934/era.2022225
Received: 02 May 2022
Revised: 24 July 2022
Accepted: 01 September 2022
Published: 13 October 2022

Research article

Reconstruction of the initial function from the solution of the fractional wave equation measured in two geometric settings

Hyungyeong Jung[1] **and Sunghwan Moon**[2,*]

[1] School of Mathematics, Kyungpook National University, Daegu 41566, Republic of Korea
[2] Department of Mathematics, College of Natural Sciences, Kyungpook National University, Daegu 41566, Republic of Korea

* **Correspondence:** Email: sunghwan.moon@knu.ac.kr.

Abstract: Photoacoustic tomography (PAT) is a novel and rapidly developing technique in the medical imaging field that is based on generating acoustic waves inside of an object of interest by stimulating non-ionizing laser pulses. This acoustic wave was measured by using a detector on the outside of the object it was then converted into an image of the human body after several inversions. Thus, one of the mathematical problems in PAT is reconstructing the initial function from the solution of the wave equation on the outside of the object. In this study, we consider the fractional wave equation and assume that the point-like detectors are located on the sphere and hyperplane. We demonstrate a way to recover the initial function from the data, namely, the solution of the fractional wave equation, measured on the sphere and hyperplane.

Keywords: photoacoustic; tomography; wave equation; fractional derivative

1. Introduction

Photoacoustic imaging (PAI) is a new biomedical imaging modality that integrates the advantages of each of the underlying modalities while complementing the problems of optical and ultrasound imaging. It is a hybrid technology that combines the high-contrast and spectroscopic-based specificity of optical imaging with the high spatial resolution of ultrasound imaging [1, 2]. PAI capitalizes on photoacoustic effects to form images of biological tissues without tissue damage. The photoacoustic effect, discovered by Alexander Graham Bell in 1880, refers to the generation of acoustic waves using thermal expansion by absorbing electromagnetic waves such as light or radio waves [3, 4].

Photoacoustic tomography (PAT) is a PAI methodology that involves irradiating a non-ionizing pulse wave within the tissue of a given object of diagnosis to obtain a photoacoustic signal in the ultrasound range (several MHz to several tens of MHz). The photoacoustic signal is an acoustic signal generated during thermal expansion that is produced by irradiating a laser on the tissue that absorbs the irradiated laser energy. The generated photoacoustic signal is received by an ultrasonic detector placed near the object. Moreover, the spatial distribution of the pulse energy absorption contains the diagnostic information; one of our goals was to obtain this distribution from the received signal. The photoacoustic signal satisfies the wave equation, and its spatial distribution is the initial function.

Regarding the measurement procedures, it is almost impossible to judge which one is best, but the use of point detectors has been studied both mathematically and experimentally. Hence, in this article, the detector was assumed to be point-shaped with a sufficiently small dimension. At the time t, the detector measures the average pressure above the surface S where the detectors are located. At this time, it can be a reasonable assumption that this average pressure is the value of a pressure wave $p(\cdot, t)$ for the small size of the transducer. Therefore, the data collected at a position of the detector on the surface S is consistent with the restriction of p to the surface S [5].

One of the mathematical problems arising in PAT is finding the initial function from the data measured on the outside of the object and the measurement data satisfying the wave equation. According to [6, Chapter 3], solutions of fractional order differential equations describe real-life situations better than corresponding integer-order differential equations. In this study, we consider the initial value problem for the fractional wave equation [7–9] as follows:

$$\begin{array}{ll} D_t^\alpha p_\alpha(\mathbf{x}, t) = -(-\Delta_{\mathbf{x}})^{\frac{\alpha}{2}} p_\alpha(\mathbf{x}, t) & (\mathbf{x}, t) \in \mathbb{R}^n \times [0, \infty),\ 1 < \alpha \leq 2 \\ p_\alpha(\mathbf{x}, 0) = f(\mathbf{x}), & \mathbf{x} \in \mathbb{R}^n \\ \partial_t p_\alpha(\mathbf{x}, t)|_{t=0} = 0, & \mathbf{x} \in \mathbb{R}^n \end{array} \tag{1.1}$$

where $-(-\Delta_{\mathbf{x}})^{\frac{\alpha}{2}}$ is the Riesz space fractional derivative of order α, as defined below, and D_t^α is the Caputo time-fractional derivative of order α, i.e.,

$$(D_t^\alpha h)(t) := (I^{m-\alpha} h^{(m)})(t), \quad m - 1 < \alpha \leq m,\ m \in \mathbb{N},$$

I^α, $\alpha \geq 0$ is the Riemann-Liouville fractional integral

$$(I^\alpha h)(t) := \begin{cases} \dfrac{1}{\Gamma(\alpha)} \displaystyle\int_0^t (t-\tau)^{\alpha-1} h(\tau) \mathrm{d}\tau, & \text{if } \alpha > 0, \\ h(t), & \text{if } \alpha = 0, \end{cases}$$

and $\Gamma(\cdot)$ is the gamma function. For $\alpha = m$, $m \in \mathbb{N}$, the Caputo fractional derivative coincides with the standard derivative of order m. For a smooth function f on $\mathbb{R}^n$ with compact support, the Riesz fractional derivative [10–13] of order α, $\alpha \geq 0$ is defined as follows:

$$\mathcal{F}(-(-\Delta_{\mathbf{x}})^{\frac{\alpha}{2}} f)(\boldsymbol{\xi}) := -|\boldsymbol{\xi}|^\alpha (\mathcal{F} f)(\boldsymbol{\xi}),$$

where $\mathcal{F}$ is the Fourier transform of a function f defined by

$$(\mathcal{F} f)(\boldsymbol{\xi}) := \int_{\mathbb{R}^n} f(\mathbf{x}) e^{-\mathrm{i}\mathbf{x}\cdot\boldsymbol{\xi}} \mathrm{d}\mathbf{x}.$$

The solution of the fractional wave equation (1.1) is given as follows:

$$p_\alpha(\mathbf{x}, t) = \frac{1}{(2\pi)^n} \int_{\mathbb{R}^n} E_\alpha(-t^\alpha |\boldsymbol{\xi}|^\alpha) e^{\mathrm{i}\boldsymbol{\xi}\cdot\mathbf{x}} \mathcal{F} f(\boldsymbol{\xi}) \mathrm{d}\boldsymbol{\xi}. \tag{1.2}$$

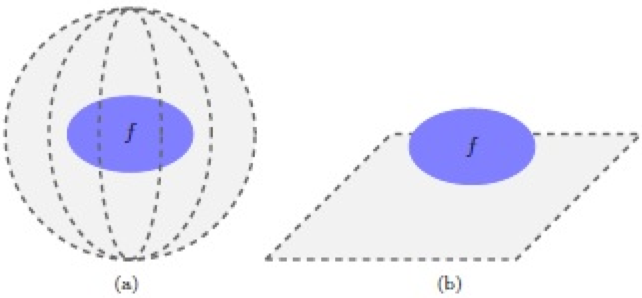

Figure 1. PAT detection geometries in $\mathbb{R}^3$: (a) spherical and (b) planar.

Here

$$E_\alpha(z) = \sum_{k=0}^{\infty} \frac{z^k}{\Gamma(1+\alpha k)}, \quad \alpha > 0,\ z \in \mathbb{C},$$

is the Mittag-Leffler function (for a more detailed explanation, see [14–16]) with

$$D_t^\alpha E_\alpha(-t^\alpha |\boldsymbol{\xi}|^\alpha) = -|\boldsymbol{\xi}|^\alpha E_\alpha(-t^\alpha |\boldsymbol{\xi}|^\alpha) \text{ and } D_t E_\alpha(-t^\alpha |\boldsymbol{\xi}|^\alpha)|_{t=0} = 0$$

from [17, Lemma 2.23]. Because $E_2(-z^2) = \cos(z)$ for $\alpha = 2$, the solution p_α of (1.1) reduces to the solution of the wave equation. Therefore, we focus on the case of $1 < \alpha < 2$ because the case of $\alpha = 2$ has been well studied in many articles [5, 18–29]. In this study, we demonstrate how to reconstruct the initial function f from the measured data, which is the solution $p_\alpha, 1 < \alpha < 2$ of the fractional wave equation (1.1) restricted to a surface with point-like detectors. To the best of our knowledge, such a PAT model has been studied here for the first time.

2. Preliminaries

Here, we consider two geometries where point-like detectors are located: spherical and hyperplanar geometries. As their names imply, in each case, detectors are located on the unit sphere and hyperplane, respectively (see Figure 1). Our goal was to reconstruct the initial function f from the measurement data, that is, the solution of (1.1) on two geometries.

In the spherical geometry, the solution p_α of (1) is measured on the unit sphere $\mathbb{S}^{n-1}$ in $\mathbb{R}^n$. Let the wave forward operator $\mathcal{W}_S$ be defined as $\mathcal{W}_S f(\boldsymbol{\theta}, t; \alpha) = p_\alpha(\boldsymbol{\theta}, t)$, $(\boldsymbol{\theta}, t) \in \mathbb{S}^{n-1} \times [0, \infty)$, where f is an initial function of (1).

Similar to the spherical geometry, the solution p_α of (1) is measured on the hyperplane $\{\mathbf{x} = (\boldsymbol{x}_*, x_n) \in \mathbb{R}^n : x_n = 0,\ \boldsymbol{x}_* \in \mathbb{R}^{n-1}\}$. Similarly, let the wave forward operator $\mathcal{W}_H$ be defined as $\mathcal{W}_H f(\boldsymbol{u}, t; \alpha) = p_\alpha(\boldsymbol{u}, t)$, $(\boldsymbol{u}, t) \in \mathbb{R}^{n-1} \times [0, \infty)$, where f is an initial function of (1).

For both geometries, the Mellin transform is essential to finding the initial function f from measurement data. Moreover, spherical harmonics are employed in the spherical geometry. The remainder of this section is devoted to introducing the Mellin transform and spherical harmonics.

Regarding the Mellin transform, the majority of the Mellin transform is derived from [34, p. 79~90].

Let f be a locally integrable function defined on $(0, \infty)$. The Mellin transform of f is defined as

$$\mathcal{M}f(s) := \int_0^\infty f(x)x^{s-1}\mathrm{d}x, \quad s \in \mathbb{C}, \tag{2.1}$$

when the integral converges. Suppose that

$$f(x) = O(x^{-a-\epsilon}) \text{ as } x \to 0^+ \quad \text{and} \quad f(x) = O(x^{-b+\epsilon}) \text{ as } x \to \infty$$

where O is the Big O notation, $\epsilon > 0$, and $a < b$. The integral (2.1) converges absolutely and defines an analytic function in the strip $a < \mathrm{Re}(s) < b$. Furthermore, its inverse transform is given by

$$f(x) = \mathcal{M}^{-1}(\mathcal{M}f)(x) = \frac{1}{2\pi\mathrm{i}}\int_{\gamma-\mathrm{i}\infty}^{\gamma+\mathrm{i}\infty} \mathcal{M}f(s)x^{-s}\mathrm{d}s, \quad \text{for} \quad a < \gamma < b.$$

Then, f can be recovered from its Mellin transform $\mathcal{M}f$ by using the inverse Mellin transform. The Mellin transform satisfies the property

$$\mathcal{M}(f \times g)(s) = \mathcal{M}f(s)\mathcal{M}g(s),$$

where the convolution is defined by

$$f \times g(x) := \int_0^\infty f(\tau)g\left(\frac{x}{\tau}\right)\frac{\mathrm{d}\tau}{\tau}. \tag{2.2}$$

Regarding the spherical harmonics, let $\boldsymbol{Y}_{lk}$ denote the spherical harmonics [30, 31] that form a complete orthonormal system in $L^2(\mathbb{S}^{n-1})$. Then, f can be expanded in the spherical harmonics as

$$f(r_{\mathbf{x}}\boldsymbol{\theta}_{\mathbf{x}}) = \sum_{l=0}^{\infty}\sum_{k=0}^{N(n,l)} f_{lk}(r_{\mathbf{x}})\boldsymbol{Y}_{lk}(\boldsymbol{\theta}_{\mathbf{x}}), \quad \text{for all} \quad f \in L^2(\mathbb{R}^n),$$

where $N(n,l) = (2l+n-2)(n+l-3)!/(l!(n-2)!)$ for $l \in \mathbb{N}$ and $N(n,0) = 1$. Moreover, we use the spherical harmonics expansions of the measurement data $\mathcal{W}_S f(\boldsymbol{\theta}, t; \alpha)$ and the Fourier transform $\mathcal{F}f(\boldsymbol{\xi})$ of the initial function f with $\boldsymbol{\xi} = \lambda_{\xi}\boldsymbol{\omega}_{\xi}$, as follows:

$$\mathcal{W}_S f(\boldsymbol{\theta}, t; \alpha) = \sum_{l=0}^{\infty}\sum_{k=0}^{N(n,l)} (\mathcal{W}_S f)_{lk}(t; \alpha)\boldsymbol{Y}_{lk}(\boldsymbol{\theta}), \quad \text{for all} \quad (t, \boldsymbol{\theta}) \in [0, \infty) \times \mathbb{S}^{n-1} \tag{2.3}$$

and

$$\mathcal{F}f(\lambda_{\xi}\boldsymbol{\omega}_{\xi}) = \sum_{l=0}^{\infty}\sum_{k=0}^{N(n,l)} (\mathcal{F}f)_{lk}(\lambda_{\xi})\boldsymbol{Y}_{lk}(\boldsymbol{\omega}_{\xi}), \quad \text{for all} \quad (\lambda_{\xi}, \boldsymbol{\omega}_{\xi}) \in [0, \infty) \times \mathbb{S}^{n-1}.$$

3. Inversion procedure

To recover the initial function, we assume that the point-like detectors are located on the unit sphere and hyperplane. Below, we provide a method to obtain the initial function f from the solution of the fractional wave equation measured on two geometries.

3.1. Spherical geometry

This section demonstrates how to obtain the initial function f from $\mathcal{W}_S f$. From (1.2), the measurement data $\mathcal{W}_S f$ are given as

$$\mathcal{W}_S f(\boldsymbol{\theta}, t; \alpha) = \frac{1}{(2\pi)^n} \int_{\mathbb{R}^n} E_\alpha(-t^\alpha |\boldsymbol{\xi}|^\alpha) e^{\mathrm{i}\boldsymbol{\xi}\cdot\boldsymbol{\theta}} \mathcal{F} f(\boldsymbol{\xi}) \mathrm{d}\boldsymbol{\xi}, \quad \text{for} \quad (\boldsymbol{\theta}, t) \in \mathbb{S}^{n-1} \times [0, \infty). \tag{3.1}$$

First, we consider a relation between $(\mathcal{W}_S f)_{lk}$ and $(\mathcal{F} f)_{lk}$.

Lemma 1. *For $f \in C^\infty(\mathbb{R}^n)$ with compact support, we have*

$$(\mathcal{W}_S f)_{lk}(t; \alpha) = \frac{\mathrm{i}^l}{(2\pi)^{\frac{n}{2}}} \int_0^\infty E_\alpha(-t^\alpha \lambda_{\boldsymbol{\xi}}^\alpha) (\mathcal{F} f)_{lk}(\lambda_{\boldsymbol{\xi}}) \lambda_{\boldsymbol{\xi}}^{\frac{n}{2}} J_{l+\frac{n-2}{2}}(\lambda_{\boldsymbol{\xi}}) \mathrm{d}\lambda_{\boldsymbol{\xi}}, \tag{3.2}$$

where $J_\nu(\cdot)$ is the Bessel function of the first kind of order ν.

Proof. Changing the variables $\boldsymbol{\xi} \to \lambda_{\boldsymbol{\xi}} \boldsymbol{\omega}_{\boldsymbol{\xi}}$ in (3.1), we write the measurement data as

$$\begin{aligned}
\mathcal{W}_S f(\boldsymbol{\theta}, t; \alpha) &= \frac{1}{(2\pi)^n} \int_{\mathbb{S}^{n-1}} \int_0^\infty E_\alpha(-t^\alpha \lambda_{\boldsymbol{\xi}}^\alpha) e^{\mathrm{i}\lambda_{\boldsymbol{\xi}} \boldsymbol{\omega}_{\boldsymbol{\xi}}\cdot\boldsymbol{\theta}} \mathcal{F} f(\lambda_{\boldsymbol{\xi}} \boldsymbol{\omega}_{\boldsymbol{\xi}}) \lambda_{\boldsymbol{\xi}}^{n-1} \mathrm{d}\lambda_{\boldsymbol{\xi}} \mathrm{d}S(\boldsymbol{\omega}_{\boldsymbol{\xi}}) \\
&= \frac{1}{(2\pi)^n} \sum_{l=0}^\infty \sum_{k=0}^{N(n,l)} \int_{\mathbb{S}^{n-1}} \int_0^\infty E_\alpha(-t^\alpha \lambda_{\boldsymbol{\xi}}^\alpha) e^{\mathrm{i}\lambda_{\boldsymbol{\xi}} \boldsymbol{\omega}_{\boldsymbol{\xi}}\cdot\boldsymbol{\theta}} (\mathcal{F} f)_{lk}(\lambda_{\boldsymbol{\xi}}) \boldsymbol{Y}_{lk}(\boldsymbol{\omega}_{\boldsymbol{\xi}}) \lambda_{\boldsymbol{\xi}}^{n-1} \mathrm{d}\lambda_{\boldsymbol{\xi}} \mathrm{d}S(\boldsymbol{\omega}_{\boldsymbol{\xi}}) \\
&= \frac{\mathrm{i}^l}{(2\pi)^{\frac{n}{2}}} \sum_{l=0}^\infty \sum_{k=0}^{N(n,l)} \int_0^\infty E_\alpha(-t^\alpha \lambda_{\boldsymbol{\xi}}^\alpha) (\mathcal{F} f)_{lk}(\lambda_{\boldsymbol{\xi}}) \lambda_{\boldsymbol{\xi}}^{\frac{n}{2}} J_{l+\frac{n-2}{2}}(\lambda_{\boldsymbol{\xi}}) \mathrm{d}\lambda_{\boldsymbol{\xi}} \boldsymbol{Y}_{lk}(\boldsymbol{\theta}),
\end{aligned}$$

where in the last line, we used the Funk-Hecke theorem [30, (3.19) in Chapter 7]:

$$\int_{\mathbb{S}^{n-1}} e^{\mathrm{i}\lambda_{\boldsymbol{\xi}} \boldsymbol{\omega}_{\boldsymbol{\xi}}\cdot\boldsymbol{\theta}} \boldsymbol{Y}_{lk}(\boldsymbol{\omega}_{\boldsymbol{\xi}}) \mathrm{d}S(\boldsymbol{\omega}_{\boldsymbol{\xi}}) = (2\pi)^{\frac{n}{2}} \mathrm{i}^l \lambda_{\boldsymbol{\xi}}^{\frac{2-n}{2}} J_{l+\frac{n-2}{2}}(\lambda_{\boldsymbol{\xi}}) \boldsymbol{Y}_{lk}(\boldsymbol{\theta}). \tag{3.3}$$

A comparison with (2.3) completes our proof. □

Now we present the main theorem:

Theorem 2. *For $f \in C^\infty(\mathbb{R}^n)$ with compact support, we have*

$$\mathcal{M}(F_{lk})(s) = 2^{\frac{n}{2}} \pi^{\frac{n-2}{2}} \alpha \mathrm{i}^{-l} \Gamma(1-s) \sin\left(\frac{\pi s}{\alpha}\right) \mathcal{M}\left[(\mathcal{W}_S f)_{lk}(\cdot; \alpha)\right](s), \quad 0 < \mathrm{Re}(s) < \alpha, \tag{3.4}$$

where

$$F_{lk}(\rho) = (\mathcal{F} f)_{lk}(\rho^{-1}) J_{l+\frac{n-2}{2}}(\rho^{-1}) \rho^{-\frac{n+2}{2}}.$$

Proof. By changing the variables $\lambda_{\boldsymbol{\xi}} \to \tilde{\lambda}_{\boldsymbol{\xi}}^{-1}$, (3.2) can be represented as

$$\begin{aligned}
(\mathcal{W}_S f)_{lk}(t; \alpha) &= \frac{\mathrm{i}^l}{(2\pi)^{\frac{n}{2}}} \int_0^\infty E_\alpha\left(-t^\alpha \tilde{\lambda}_{\boldsymbol{\xi}}^{-\alpha}\right) (\mathcal{F} f)_{lk}\left(\tilde{\lambda}_{\boldsymbol{\xi}}^{-1}\right) J_{l+\frac{n-2}{2}}\left(\tilde{\lambda}_{\boldsymbol{\xi}}^{-1}\right) \tilde{\lambda}_{\boldsymbol{\xi}}^{-\frac{n+4}{2}} \mathrm{d}\tilde{\lambda}_{\boldsymbol{\xi}} \\
&= \frac{\mathrm{i}^l}{(2\pi)^{\frac{n}{2}}} F_{lk} \times E(t; \alpha),
\end{aligned} \tag{3.5}$$

where

$$E(\rho;\alpha) = E_\alpha(-\rho^\alpha). \tag{3.6}$$

To check that the Mellin transform of $(\mathcal{W}_S f)_{lk}(\cdot;\alpha)$ in (3.5) is well-defined, it suffices to check that the Mellin transforms of F_{lk} and E are well-defined, respectively. Let us consider the Mellin transform of F_{lk}. Notice that

$$F_{lk}(\rho) = O(\rho^\infty) \text{ as } \rho \to 0^+ \quad \text{and} \quad F_{lk}(\rho) = O(\rho^{-l-n}) \text{ as } \rho \to \infty,$$

because $J_\nu(\tilde{\rho}) = O(\tilde{\rho}^\nu)$ as $\tilde{\rho} \to 0^+$ [32]. Therefore, $\mathcal{M}(F_{lk})(s)$ is well-defined for $\mathrm{Re}(s) < l + n - \epsilon$ for any $\epsilon > 0$. Next, we consider the Mellin transform of E. Taking the Mellin transform of E, we obtain the following formula (see [33, Lemma 9.1] or [15, (2.18)]): for $0 < \mathrm{Re}(s) < \alpha$

$$\mathcal{M}(E_\alpha(-\cdot))(s) = \int_0^\infty E_\alpha(-\rho)\rho^{s-1}\mathrm{d}\rho = \frac{\Gamma(s)\Gamma(1-s)}{\Gamma(1-\alpha s)}.$$

Hence, we have

$$\mathcal{M}(E)(s;\alpha) = \int_0^\infty E(\rho;\alpha)\rho^{s-1}\mathrm{d}\rho = \frac{\Gamma\left(\frac{s}{\alpha}\right)\Gamma\left(1-\frac{s}{\alpha}\right)}{\alpha\Gamma(1-s)} = \frac{\pi}{\alpha\Gamma(1-s)\sin(\frac{\pi s}{\alpha})}, \tag{3.7}$$

where in the third equality, we applied the Euler's reflection formula $\Gamma(p)\Gamma(1-p) = \dfrac{\pi}{\sin(\pi p)}$. Thus, the Mellin transform of (3.5) is well-defined for $0 < \mathrm{Re}(s) < \alpha$. Taking the Mellin transforms on both sides of (3.5), we have

$$\mathcal{M}\left[(\mathcal{W}_S f)_{lk}(\cdot;\alpha)\right](s) = \frac{\mathrm{i}^l}{(2\pi)^{\frac{n}{2}}}\mathcal{M}(F_{lk})(s)\mathcal{M}(E)(s;\alpha) = \frac{\pi \mathrm{i}^l}{(2\pi)^{\frac{n}{2}}\alpha}\frac{\mathcal{M}(F_{lk})(s)}{\Gamma(1-s)\sin\left(\frac{\pi s}{\alpha}\right)},$$

where in the second equality, we used (3.7). □

Now, taking the inverse Mellin transform of $\mathcal{M}\left[(\mathcal{W}_S f)_{lk}(\cdot;\alpha)\right](s)$, we can reconstruct F_{lk} and $(\mathcal{F}f)_{lk}$.

Corollary 3. *For $f \in C^\infty(\mathbb{R}^n)$ with compact support, we reconstruct f_{lk} from $(\mathcal{W}_S f)_{lk}$ by recovering the F_{lk} :*

$$(\mathcal{F}f)_{lk}(\rho) = 2^{\frac{n}{2}}\pi^{\frac{n-2}{2}}\alpha \mathrm{i}^{-l}\mathcal{M}^{-1}\left[\Gamma(1-\cdot)\sin\left(\frac{\pi\cdot}{\alpha}\right)\mathcal{M}\left[(\mathcal{W}_S f)_{lk}\right](\cdot;\alpha)\right](\rho^{-1})J_{l+\frac{n-2}{2}}(\rho)^{-1}\rho^{-\frac{n+2}{2}}.$$

Thus far, we have considered the measurement data $\mathcal{W}_S f$. Note that our approach can be applied to the direction dependent measurement data from the model in [29] as well.

Remark 4. *For $f \in C^\infty(\mathbb{R}^n)$ with compact support, let*

$$g(\boldsymbol{\theta},t;\alpha) = c_1\mathcal{W}_S f(\boldsymbol{\theta},t;\alpha) + c_2\left[\boldsymbol{\theta}\cdot\nabla_{\mathbf{x}}\mathcal{W}_S f(\mathbf{x},t;\alpha)\right]_{\mathbf{x}=\boldsymbol{\theta}}, \quad (\boldsymbol{\theta},t) \in \mathbb{S}^{n-1}\times[0,\infty)$$

be the direction dependent measurement data modeled as described in [29, (1.2)], where $\boldsymbol{\theta} \cdot \nabla_{\mathbf{x}} \mathcal{W}_S f$ *is the normal derivative of* $\mathcal{W}_S f$ *and* c_1 *and* $c_2 \in \mathbb{R}$ *are constants. Using* (2.3), (3.3), *and the Bessel function identity* $\frac{\mathrm{d}}{\mathrm{d}\lambda}\left[\lambda^{-\nu} J_\nu(\lambda)\right] = -\lambda^{-\nu} J_{\nu+1}(\lambda)$ *(see, [32, (5.13) on pp. 133]), we obtain* g_{lk}*:*

$$\begin{aligned} g_{lk}(t;\alpha) &= \frac{\mathrm{i}^l}{(2\pi)^{\frac{n}{2}}} \int_0^\infty E_\alpha(-t^\alpha \lambda^\alpha)(\mathcal{F} f)_{lk}(\lambda)\lambda^{\frac{n}{2}} \left[(c_1 + c_2 l) J_{l+\frac{n-2}{2}}(\lambda) - c_2 \lambda J_{l+\frac{n}{2}}(\lambda)\right] \mathrm{d}\lambda \\ &= \frac{\mathrm{i}^l}{(2\pi)^{\frac{n}{2}}} F_{lk} \times E(t;\alpha), \end{aligned} \tag{3.8}$$

where we used (3.6) *and*

$$F_{lk}(\rho) = (\mathcal{F} f)_{lk}(\rho^{-1})\rho^{-\frac{n+2}{2}} \left[(c_1 + c_2 l) J_{l+\frac{n-2}{2}}(\rho^{-1}) - c_2(\rho^{-1}) J_{l+\frac{n}{2}}(\rho^{-1})\right].$$

By taking the Mellin transform on both sides of (3.8)*, and because* $\mathcal{M}(g_{lk})$ *is well-defined for* $0 < \mathrm{Re}(s) < \alpha$*, we have* $\mathcal{M}(F_{lk})$:

$$\mathcal{M}(F_{lk})(s) = 2^{\frac{n}{2}} \pi^{\frac{n}{2}-1} \alpha \mathrm{i}^{-l} \Gamma(1-s) \sin\left(\frac{\pi s}{\alpha}\right) \mathcal{M}(g_{lk})(s).$$

Moreover, using the inverse Mellin transform of $\mathcal{M}(F_{lk})$*, we can recover* F_{lk}*,* $\mathcal{F} f_{lk}$*, and* f *from the Mellin transform* $\mathcal{M}(F_{lk})$*.*

3.2. Hyperplanar geometry

Similar to the previous subsection, Section 3.1, we show that f can be determined from $\mathcal{W}_H f$. From (1.2), the measurement data $\mathcal{W}_H f$ are given as follows:

$$\mathcal{W}_H f(\boldsymbol{u}, t;\alpha) = \frac{1}{(2\pi)^n} \int_{\mathbb{R}^{n-1}} \int_{\mathbb{R}} E_\alpha\left(-t^\alpha \left|(\boldsymbol{\xi}_*, \xi_n)\right|^\alpha\right) e^{\mathrm{i}\boldsymbol{u}\cdot\boldsymbol{\xi}_*} \mathcal{F} f(\boldsymbol{\xi}_*, \xi_n) \mathrm{d}\xi_n \mathrm{d}\boldsymbol{\xi}_*, \tag{3.9}$$

for $(\boldsymbol{u}, t) \in \mathbb{R}^{n-1} \times [0,\infty)$. If f is odd in x_n, then $\mathcal{W}_H f(\boldsymbol{u}, t;\alpha) = 0$. Thus we assume that f is even in x_n. First, we analyze the analog of the Fourier slice theorem:

Lemma 5. *For* $f \in C^\infty(\mathbb{R}^n)$ *with compact support and that is even in* x_n*, we have*

$$\mathcal{F}_{\boldsymbol{u}}(\mathcal{W}_H f)(\boldsymbol{\eta}_*, t;\alpha) = \frac{1}{\pi} \int_0^\infty E_\alpha(-t^\alpha \lambda^\alpha) \mathcal{F} f\left(\boldsymbol{\eta}_*, \sqrt{\lambda^2 - |\boldsymbol{\eta}_*|^2}\right) \frac{\lambda \chi_{|\boldsymbol{\eta}_*| \le \lambda}(\lambda)}{\sqrt{\lambda^2 - |\boldsymbol{\eta}_*|^2}} \mathrm{d}\lambda. \tag{3.10}$$

The Lemma for $\alpha = 2$ has already been studied in [18, 23, 25].

Proof. Taking the $n-1$-dimensional Fourier transform of $\mathcal{W}_H f$ defined in (3.9) with respect to $\boldsymbol{u}$, we have

$$\begin{aligned} \mathcal{F}_{\boldsymbol{u}}(\mathcal{W}_H f)(\boldsymbol{\eta}_*, t;\alpha) &= \frac{1}{2\pi} \int_{\mathbb{R}} E_\alpha\left(-t^\alpha \left|(\boldsymbol{\eta}_*, \xi_n)\right|^\alpha\right) \mathcal{F} f(\boldsymbol{\eta}_*, \xi_n) \mathrm{d}\xi_n \\ &= \frac{1}{\pi} \int_0^\infty E_\alpha\left(-t^\alpha \left|(\boldsymbol{\eta}_*, \xi_n)\right|^\alpha\right) \mathcal{F} f(\boldsymbol{\eta}_*, \xi_n) \mathrm{d}\xi_n \\ &= \frac{1}{\pi} \int_0^\infty E_\alpha(-t^\alpha \lambda^\alpha) \mathcal{F} f\left(\boldsymbol{\eta}_*, \sqrt{\lambda^2 - |\boldsymbol{\eta}_*|^2}\right) \frac{\lambda \chi_{|\boldsymbol{\eta}_*| \le \lambda}(\lambda)}{\sqrt{\lambda^2 - |\boldsymbol{\eta}_*|^2}} \mathrm{d}\lambda \end{aligned}$$

where in the second line, we used the evenness of $\mathcal{F}f$ and E_α with respect to the last variable ξ_n, and in the last line, we changed the variables $\left|(\boldsymbol{\eta}_*, \xi_n)\right| \to \lambda$. □

Now we present the main theorem:

Theorem 6. *For $f \in C^\infty(\mathbb{R}^n)$ with compact support and that is even in x_n, we have*

$$\mathcal{M}(F_{\boldsymbol{\eta}_*})(s) = \alpha\Gamma(1-s)\sin\left(\frac{\pi s}{\alpha}\right)\mathcal{M}\left[\mathcal{F}_{\boldsymbol{u}}(\mathcal{W}_H f)\right](\boldsymbol{\eta}_*, s; \alpha), \quad 0 < \mathrm{Re}(s) < \alpha$$

where

$$F_{\boldsymbol{\eta}_*}(\lambda) = \mathcal{F}f(\boldsymbol{\eta}_*, \sqrt{\lambda^{-2} - \left|\boldsymbol{\eta}_*\right|^2})\frac{\chi_{|\boldsymbol{\eta}_*| \le \lambda^{-1}}(\lambda^{-1})}{\lambda^2\sqrt{\lambda^{-2} - \left|\boldsymbol{\eta}_*\right|^2}}.$$

Proof. By changing the variables $\lambda \to \tilde{\lambda}^{-1}$, (3.10) can be represented as

$$\begin{aligned}\mathcal{F}_{\boldsymbol{u}}(\mathcal{W}_H f)(\boldsymbol{\eta}_*, t; \alpha) &= \frac{1}{\pi}\int_0^\infty E_\alpha\left(-t^\alpha\tilde{\lambda}^{-\alpha}\right)\mathcal{F}f(\boldsymbol{\eta}_*, \sqrt{\tilde{\lambda}^{-2} - \left|\boldsymbol{\eta}_*\right|^2})\frac{\chi_{|\boldsymbol{\eta}_*| \le \tilde{\lambda}^{-1}}(\tilde{\lambda}^{-1})}{\tilde{\lambda}^3\sqrt{\tilde{\lambda}^{-2} - \left|\boldsymbol{\eta}_*\right|^2}}\mathrm{d}\tilde{\lambda} \\ &= \frac{1}{\pi}F_{\boldsymbol{\eta}_*} \times E(t; \alpha),\end{aligned}$$

where in the second line, we used the convolution (2.2) and (3.6). To demonstrate that the Mellin transform of $\mathcal{F}_{\boldsymbol{u}}(\mathcal{W}_H f)$ defined is well-defined, we only need to check that the Mellin transforms of $F_{\boldsymbol{\eta}_*}$ are well-defined because, by Theorem 2 $\mathcal{M}(E)$ is well-defined for $0 < \mathrm{Re}(s) < \alpha$. Notice that

$$F_{\boldsymbol{\eta}_*}(\lambda) = O(\lambda^\infty) \text{ as } \lambda \to 0^+ \quad \text{and} \quad F_{\boldsymbol{\eta}_*}(\lambda) = O(\lambda^{-\infty}) \text{ as } \lambda \to \infty,$$

Therefore, $\mathcal{M}\left(F_{\boldsymbol{\eta}_*}\right)(s)$ is well-defined for any $s \in \mathbb{C}$ and the Mellin transform of $\mathcal{F}_{\boldsymbol{u}}(\mathcal{W}_H f)(s)$ is well-defined for $0 < \mathrm{Re}(s) < 2$. Taking the Mellin transform, we have

$$\mathcal{M}\left[\mathcal{F}_{\boldsymbol{u}}(\mathcal{W}_H f)\right](\boldsymbol{\eta}_*, s; \alpha) = \frac{1}{\pi}\mathcal{M}(F_{\boldsymbol{\eta}_*})(s)\mathcal{M}(E)(s; \alpha) = \frac{\mathcal{M}(F_{\boldsymbol{\eta}_*})(s)}{\alpha\Gamma(1-s)\sin\left(\frac{\pi s}{\alpha}\right)},$$

where in the second equality, we used (3.7). □

Again, taking the inverse Mellin transform of $\mathcal{M}(F_{\boldsymbol{\eta}_*})(s)$, we reconstruct F_{lk} and $(\mathcal{F}f)_{lk}$.

Corollary 7. *For $f \in C^\infty(\mathbb{R}^n)$ with compact support and that is even in x_n, we reconstruct $\mathcal{F}f$ from $\mathcal{W}_H f$ by recovering the $F_{\boldsymbol{\eta}_*}$; accordingly, for $\boldsymbol{\eta} = (\boldsymbol{\eta}_*, \eta_n) \in \mathbb{R}^{n-1} \times \mathbb{R}$,*

$$\mathcal{F}f(\boldsymbol{\eta}) = \frac{\eta_n}{|\boldsymbol{\eta}|^2}\mathcal{M}^{-1}\left[\alpha\Gamma(1-\cdot)\sin\left(\frac{\pi\cdot}{\alpha}\right)\mathcal{M}\left[\mathcal{F}_{\boldsymbol{u}}(\mathcal{W}_H f)\right](\boldsymbol{\eta}_*, \cdot; \alpha)\right](|\boldsymbol{\eta}|^{-1}).$$

4. Conclusions

Recovering the initial function f from the solutions of the wave equation on some surface surrounding the object is crucial for the recently developed PAT methodology. In this study, we first investigated one mathematical problem of PAT by using the fractional wave equation in order to provide a way for to reconstruct f from fractional wave equation solutions restricted to the sphere and hyperplane.

We summarize both cases as follows:

For the spherical case, we can recover f from $\mathcal{W}_S f$ through the following steps:

1) Find $(\mathcal{W}_S f)_{lk}$ using the spherical harmonics (see Lemma 1).
2) Take the Mellin transform of $(\mathcal{W}_S f)_{lk}$.
3) From Theorem 2, we obtain $\mathcal{M}(F_{lk})$ from $\mathcal{M}[(\mathcal{W}_S f)_{lk}]$.
4) Taking the inverse Mellin transform, we recover F_{lk} from the Mellin transform $\mathcal{M}(F_{lk})$ (see Corollary 3).
5) Next, we find $(\mathcal{F} f)_{lk}$ from F_{lk} and finally get f.

For the hyperplane case, we can recover f from $\mathcal{W}_H f$ through the following steps:

1) Take the $n-1$-dimensional Fourier transform of $\mathcal{W}_H f$ to get $\mathcal{F}_{\boldsymbol{u}}(\mathcal{W}_H f)$ (see Lemma 5).
2) Take the Mellin transform of $\mathcal{F}_{\boldsymbol{u}}(\mathcal{W}_H f)$.
3) Using Theorem 6, we find $\mathcal{M}(F_{\eta_*})$ from $\mathcal{M}[\mathcal{F}_{\boldsymbol{u}}(\mathcal{W}_H f)]$.
4) Taking the inverse Mellin transform, we recover F_{η_*} from the Mellin transform $\mathcal{M}(F_{\eta_*})$ (see Corollary 7).
5) Next, we find $\mathcal{F} f$ from F_{η_*} and finally get f.

Acknowledgements

The authors are thankful to the referees for their multiple suggestions that helped to improve this paper. We would like to thank Editage (www.editage.co.kr) for English language editing. This study was supported by a National Research Foundation of Korea grant (MSIP) and the Basic Science Research Program through the National Research Foundation of Korea (NRF) funded by the South Korean government (NRF-2022R1C1C1003464, NRF-2020R1F1A1A01065912, NRF-2020R1A4A1018190). This work was conducted as H. Jung's Master's thesis.

Conflict of interest

This study does not have any conflicts of interest.

References

1. P. Beard, Biomedical photoacoustic imaging, *Interface focus*, **1** (2011), 602–631. https://doi.org/10.1098/rsfs.2011.0028
2. H. Jiang, *Photoacoustic Tomography*, 1st Edition, CRC Press, 2018. https://doi.org/10.1201/9781315213903

3. C. L. Bayer, G. P. Luke, S. Y. Emelianov, Photoacoustic imaging for medical diagnostics, *Acoust. Today*, **8** (2012), 15–23. https://doi.org/10.1121/1.4788648
4. A. G. Bell, On the production and reproduction of sound by light, *Amer. J. Sci.*, **20** (1880), 305–324. https://doi.org/10.2475/ajs.s3-20.118.305
5. P. Kuchment, The radon transform and medical imaging, *Society Indust. Appl. Math.*, 2013.
6. R. Hilfer, P. L. Butzer, U. Westphal, An introduction to fractional calculus, in *Applications of Fractional Calculus in Physics*, World Scientific, (2010), 1–85.
7. L. Boyadjiev, Y. Luchko, Multi-dimensional α-fractional wave equation and some properties of its fundamental solution, *Comput. Math. Appl.*, **73** (2017), 2561–2572. https://doi.org/10.1016/j.camwa.2017.03.020
8. L. Boyadjiev, Y. Luchko, Mellin integral transform approach to analyze the multi-dimensional diffusion-wave equations, *Chaos, Solitons Fractals*, **102** (2017), 127–134. https://doi.org/10.1016/j.chaos.2017.03.050
9. Y. Luchko, On some new properties of the fundamental solution to the multi-dimensional space-and time-fractional diffusion-wave equation, *Mathematics*, **5** (2017), 76. https://doi.org/10.3390/math5040076
10. P. Chen, R. Wang, X. Zhang, Long-time dynamics of fractional nonclassical diffusion equations with nonlinear colored noise and delay on unbounded domains, *Bull. des Sci. Math.*, **173** (2021), 103071. https://doi.org/10.1016/j.bulsci.2021.103071
11. E. D. Nezza, G. Palatucci, E. Valdinoci, Hitchhiker's guide to the fractional Sobolev spaces, *Bull. des Sci. Math.*, **136** (2012), 521–573. https://doi.org/10.1016/j.bulsci.2011.12.004
12. A. I. Saichev, G. M. Zaslavsky, Fractional kinetic equations: Solutions and applications, *Chaos An Interdiscip. J. Nonlinear Sci.*, **7** (1997), 753–764. https://doi.org/10.1063/1.166272
13. S. G. Samko, A. A. Kilbas, O. I. Marichev, *Fractional Integrals and Derivatives-theory and Applications Gordon and Breach*, Linghorne, PA, 1993.
14. K. Górska, A. Lattanzi, G Dattoli, Mittag-Leffler function and fractional differential equations, *Fract. Calc. Appl. Anal.*, **21** (2018), 220–236. https://doi.org/10.1515/fca-2018-0014
15. Y. Luchko, V. Kiryakova. The mellin integral transform in fractional calculus, *Fract. Calc. Appl. Anal.*, **16** (2013), 405–430. https://doi.org/10.2478/s13540-013-0025-8
16. Y. Luchko, Operational calculus for the general fractional derivative and its applications, *Fract. Calc. Appl. Anal.*, **24** (2021), 338–375. https://doi.org/10.1515/fca-2021-0016
17. A. A. Kilbas, H. M. Srivastava, J. J. Trujillo, *Theory and Applications of Fractional Differential Equations*, Elsevier, 2006.
18. M. A. Anastasio, J. Zhang, D. Modgil, P. J. La Rivière, Application of inverse source concepts to photoacoustic tomography, *Inverse Probl.*, **23** (2007), S21. https://doi.org/10.1088/0266-5611/23/6/S03
19. A. L. Bukhgeim, V. B. Kardakov, Solution of the inverse problem for the equation of elastic waves by the method of spherical means, *Siberian Math. J.*, **19** (1978), 528–535. https://doi.org/10.1007/BF00967723

20. N. Do, L. Kunyansky, Theoretically exact photoacoustic reconstruction from spatially and temporally reduced data, *Inverse Probl.*, **34** (2018), 094004. https://doi.org/10.1088/1361-6420/aacfac

21. F. Dreier, M. Haltmeier, Explicit inversion formulas for the two-dimensional wave equation from neumann traces, *SIAM J. Imaging Sci.*, **13** (2020), 589-608. https://doi.org/10.1137/19M1260517

22. D. Finch, M. Haltmeier, Rakesh, Inversion of spherical means and the wave equation in even dimensions, *SIAM J. Appl. Math.*, **68** (2007), 392–412. https://doi.org/10.1137/070682137

23. K. Köstli, M. Frenz, H. Bebie, H. Weber, Temporal backward projection of optoacoustic pressure transients using fourier transform methods, *Phys. Med. Biol.*, **46** (2001), 1863. https://doi.org/10.1088/0031-9155/46/7/309

24. L. A. Kunyansky, Fast reconstruction algorithms for the thermoacoustic tomography in certain domains with cylindrical or spherical symmetries, *Inverse Probl. Imag.*, **6** (2012),111–131. https://doi.org/10.3934/ipi.2012.6.111

25. S. Moon, Inversion formulas and stability estimates of the wave operator onthehyperplane, *J. Math. Anal. Appl.*, **466** (2018), 490–497. https://doi.org/10.1016/j.jmaa.2018.06.006

26. E. K. Narayanan, Rakesh, Spherical means with centers on a hyperplane in even dimensions, *Inverse Probl.*, **26** (2010), 035014. https://doi.org/10.1088/0266-5611/26/3/035014

27. G. Thummerer, G. Mayr, M. Haltmeier, P. Burgholzer, Photoacoustic reconstruction from photothermal measurements including prior information, *Photoacoustics*, **19** (2020), 100175. https://doi.org/10.1016/j.pacs.2020.100175

28. M. Xu, L, Wang, Universal back-projection algorithm for photoacoustic computed tomography, *Phys. Rev. E* , **71** (2005), 016706.https://doi.org/10.1103/PhysRevE.71.016706

29. G. Zangerl, S. Moon, M. Haltmeier, Photoacoustic tomography with direction dependent data: an exact series reconstruction approach, *Inverse Probl.*, **35** (2019), 114005. https://doi.org/10.1088/1361-6420/ab2a30

30. F. Natterer, *The mathematics of computerized tomography*, Soc. Ind. Appl. Math., 2001. https://doi.org/10.1137/1.9780898719284

31. R. T. Seeley, Spherical harmonics, *Am. Math. Mon.*, **73** (1996), 115–121. https://doi.org/10.1080/00029890.1966.11970927

32. G. B. Folland, *Fourier Analysis and Its Applications*, American Mathematical Soc, 2009.

33. H. J. Haubold, A. M. Mathai, R. K. Saxena, Mittag-Leffler functions and their applications, *J. Appl. Math.*, **2011**, (2011). https://doi.org/10.1155/2011/298628

34. R. B. Paris, D. Kaminski, *Asymptotics and Mellin-Barnes Integrals*, Cambridge University Press, 2001. https://doi.org/10.1017/CBO9780511546662

AIMS Press

© 2022 the Author(s), licensee AIMS Press. This is an open access article distributed under the terms of the Creative Commons Attribution License (http://creativecommons.org/licenses/by/4.0)